Meteorologische Zeitschrift, Vol. **20**, No. 4, 431-440 (June 2011)

Open Access Article

Application of ground-based, multi-channel microwave radiometer in the nowcasting of intense convective weather through instability indices of the atmosphere

P.W. Chan* and K.K. Hon

Hong Kong Observatory, Hong Kong, China

(Manuscript received December 25, 2010; in revised form May 1, 2011; accepted May 2, 2011)

Abstract

A ground-based microwave radiometer gives the possibility of providing continuously available temperature and humidity profiles of the troposphere, from which instability indices of the atmosphere could be derived. This paper studies the possibility of correlating the radiometer-based instability indices with the occurrence of intense convective activity, namely, the occurrence of lightning. The correlation so established could be useful for the nowcasting of convective weather: the weather forecaster follows the evolution of the radiometer-based instability indices in order to access the chance for lightning to occur. The quality of the radiometer-based instability indices is first established by comparing with the radiosonde-based indices. Though there are biases and spreads in the scatter plots of the two datasets, the radiometer-based indices appear to follow the trend of the radiosonde-based indices in spite of the differences in measurement locations and working principles of the two instruments. The thresholds of instability indices for the occurrence of lightning (using 1 discharge) are then determined, specifically for the radiometer in use and the climatological condition in Hong Kong. It turns out that, among all the indices considered in this paper, KI has the best performance in terms of probability of detection of lightning occurrence, particularly for non-summer months, by using an optimum threshold. Finally, the correlation between the instability index and the amount of lightning strokes (within a certain distance from the radiometer) is established. It turns out that the correlation is the best using the minimum value of humidity index, with correlation coefficient of 0.55. The distance from the radiometer considered is about 30 km (having the best correlation between the number of lightning discharges and the instability index), which may be taken as the area over which the radiometer's measurement is considered to be representative of the atmospheric conditions.

Zusammenfassung

Bodengestützte Mikrowellen-Radiometer geben die Möglichkeit, kontinuierliche Profildaten für Temperatur und Feuchte bereit zu stellen, aus welchen Instabilitätsindizes für die Atmosphäre abgeleitet werden können. Hier soll die Möglichkeit der Korrelation von radiometer-basierten Instabilitätsindizes mit dem Auftreten von konvektiver Aktivität (Blitzen) untersucht werden. Solche Korrelationen könnten für das Nowcasting von konvektiven Wettererscheinungen nützlich sein: der Beobachter könnte aus der zeitlichen Entwicklung dieser Indizes auf die Wahrscheinlichkeit des Auftretens von Blitzen schließen. Zunächst wird die Qualität dieser Indizes mit solchen aus Radiosondendaten verglichen. Trotz systematischen Abweichungen und Streuungen scheinen diese Indizes denen aus den Radiosondendaten zu folgen. Dies geschieht, obwohl eine räumliche Distanz und prinzipielle Unterschiede zwischen den beiden Messsystemen bestehen. Danach werden Schwellenwerte für die Indizes bestimmt, die für die klimatologischen Gegebenheiten Hongkongs gelten. Es stellt sich heraus, dass der KI-Index die beste Fähigkeit hat, das Auftreten von Blitzen vorherzusagen, insbesondere für die Nicht-Sommer-Monate. Schließlich wird eine Korrelation zwischen den Index-Werten und der Blitzzahl untersucht. Hier zeigt sich mit 0,55 die beste Korrelation mit dem Minimalwert des Feuchteindex. Aus der Korrelation mit der Blitzzahl kann gefolgert werden, dass die Radiometerwerte für einen Umkreis von ca. 30 km für die atmosphärischen Bedingungen repräsentativ sind.

1 Introduction

Instability indices derived from the thermodynamic profiles of the atmosphere could be useful in the forecasting and nowcasting of intense convective weather. Traditionally, such indices are obtained from the upper-air ascent data as measured by, for instance, radiosondes. However, such data are only available a few times a day, and thus they are not frequent enough to capture the rapid variability of the thermodynamic state of the atmosphere.

Ground-based microwave radiometers provide an alternative source of thermodynamic profiles of the atmosphere. In microwave remote-sensing of the atmosphere, the characteristics of microwave radiations depend on the absorption of the waves by the atmosphere. According to the modern light theory and experimental results, the major absorbing matters of microwave radiations in the atmosphere include water vapour, oxygen, cloud liquid water and precipitation. There are two absorption bands of microwave radiations by water vapour in the frequency range of 10 to 220 GHz, namely, near 22 and 183 GHz. The absorption bands of oxygen occur in the

*Corresponding author: P.W. Chan, Hong Kong Observatory, 134A Nathan Road, Kowloon, Hong Kong, China, email: pwchan@hko.gov.hk

DOI 10.1127/0941-2948/2011/0276

0941-2948/2011/0276 $ 4.50

region near 60 and 119 GHz. The absorption of the microwave radiations by cloud liquid water is continuous across the 10–220 GHz spectrum. According to Kirchhoff's law, a radiator that has the strongest absorption in a frequency band also has the strongest emission in that band. As a result, the changes of the microwave radiations in the frequency region around 22.235 GHz mainly reflect the evolution of atmospheric water vapour density. Similarly, the radiation changes in the strong absorption bands of oxygen near 60 GHz show the evolution of atmospheric temperature, and those occurring in the frequency band near 31.5 GHz are mainly related to the evolution of the liquid water paths inside clouds. Based on the above principles, the microwave radiometer working in the above-described frequency bands could be used to measure the vertical profiles of temperature, water vapour and liquid water in the atmosphere.

The major limitations of the microwave remote-sensing technology include: (i) the retrieval of temperature and humidity profiles need to be made based on historical data of long period, such as radiosonde ascent data of similar climatological conditions over many years; (ii) the emitted radiations at the middle and the upper troposphere are rather weak, and thus there would be higher uncertainty with the retrieved temperature and humidity values; (iii) rain water accumulation on the radome of the radiometer may affect the measurement accuracy. Despite such limitations, there have been improvements in the microwave radiometry technology in the recent years. Even though the radiometer's retrieved profiles may not appear to be identical to the profiles obtained from the nearby radiosonde accents (which are still taken to be the sky truth), both datasets have been found to give similar trends in the evolution of the temperature and the humidity inside the troposphere.

There have been many studies of correlating convective activity with the radiosonde-derived instability indices, such as MANZATO (2003), MARINAKI et al. (2006) and TUDURÍ and RAMIS (1997). The purpose of such studies is that, when radiosonde-based instability indices are available in the operational weather forecasting service, the weather forecasters could assess the chance of occurrence of intense convective weather in the region of interest. However, such studies are limited by the temporal resolution of the radiosonde data, which are only available two times to four times a day. On the other hand, microwave radiometers basically give nearly continuous measurements of the temperature and humidity profiles, from the ground up to a height of 10 km. The radiometer-derived instability indices could be useful in monitoring the chance of the occurrence of intense convective weather, once the correlation between the instability indices and the occurrence of convective weather is established. The weather forecasters could monitor the continuously available radiometer-derived instability indices in real time to assess the chance of thunderstorms and lightning. Of course, one has to note the limitation of the accuracy of the radiometer measurements. For the radiometer under consideration (RPG-HATPRO from Radiometer Physics GmbH, with manual available at www.radiometer-physics.de/rpg/html/Download.html), it has been specified that the temperature accuracy is in the order of 1 to 2 degrees K, and the relative humidity has an accuracy of 10–20 % (according to unpublished notes from the manufacturer for studies of the radiometer based on comparison with tower measurements). There may be bias and deviations of the radiometer measurements from the nearby radiosonde data at the same time. However, as long as the two datasets show similar trends in the measurements of temperature and humidity, the radiometer data could take up the role of radiosonde in providing the time series of instability indices for the purpose of nowcasting the occurrence of intense convective weather.

Preliminary study of radiometer-based instability indices has been presented in CHAN (2009). However, in that study, only the data of one summer are considered. The present paper gives the result over a longer period, namely, over a whole year, and aims at looking at the following aspects of the radiometer-based indices:

(a) To establish the quality of the radiometer-based indices by comparing with the radiosonde-derived indices;

(b) To find out if the conventional thresholds for convective weather as adopted for the various indices are applicable for the climatological condition in Hong Kong, using lightning occurrence as a proxy of the convective weather;

(c) To find out the seasonal variation of the thresholds as discussed in (b) above, and to determine which indices have the best correlation with the occurrence of lightning; and

(d) To establish quantitative correlation, if any, between the instability index and the number of lightning strokes within a certain distance from the radiometer.

(e) The above analysis is carried out for the climatological condition in Hong Kong based on data of one year.

2 Instability indices under consideration

The instability indices considered in the present study consist of a number of types, namely:

(a) indices depending on the temperature and dew point at specific heights only, such as K index (KI),

$KI = (T_{850} - T_{500}) + Td_{850} - (T_{700} - Td_{700})$

where T is the temperature, Td is the dew point, and the subscript refers to the pressure levels; as this index increases from a value of 20 or so, the likelihood of showers and thunderstorms is expected to increase (based

on AMS Glossary, http://amsglossary.allenpress.com/glossary); humidity index (HI)
$HI = (T - Td)_{850} + (T - Td)_{700} + (T - Td)_{500}$
this index has been considered, for instance, in MICHALOPOULOU and JACOVIDES (1987), in which the criterion HI≤30 is used in the forecasting of thundestorms; and total totals index (TT)
$TT = T_{850} + Td_{850} - 2T_{500}$
according to AMS Glossary, showers and thunderstorms become increasingly likely from TT values of about 30, and severe thunderstorms are considered likely for values of 50 or more.

(b) an index relating to the energy available for convection, namely, Convective Available Potential Energy (CAPE), which is the area bound by the temperature profile of the atmosphere and the saturated adiabatic lapse rate in the tephigram,

$$CAPE = \int_{p_n}^{p_f} (\alpha_p - \alpha_e) dp$$

where α_e is the environmental specific volume profile, α_p is the specific volume of a parcel moving upward moist-adiabatically from the level of free convection, p_f is the pressure at the level of free convection, and p_n is the pressure at the level of neutral buoyancy; in the literature, there does not seem to be a definite threshold of CAPE for thunderstorm occurrence, and it is generally considered that thunderstorm may occur when CAPE reaches several thousands or more;

(c) an index relating to the curvature of the equivalent potential energy profile of the atmosphere, namely, the shape factor, SF (WALKER et al., 2008):

$$SF = \left|\frac{1}{T_F - T_0}\right| \int_{Z_0}^{Z_F} \frac{d\theta_E}{dz} \sqrt{1 + (\alpha\beta\frac{d^2\theta_E}{dz^2})^2}\, dz$$

where T is absolute temperature, z is height, and Θ_E is the equivalent potential temperature; subscript F is the highest point in the profile, subscript 0 is the surface; and α and β are scaling factors depending on z_F, z_0, T_F and T_0. According to WALKER et al. (2008), the threshold for distinguishing between rain-free weather and severe weather would be –30, at least for the climatological condition of the place under consideration in that study.

In the present study, the radiometer's temperature and humidity data are used to calculate the various instability indices. It is possible to retrieve the index directly from the raw brightness temperature measurements of the radiometer by establishing the relevant retrieval algorithms (statistical methods), but it may be possible to have inconsistency among the various radiometer-derived instability indices using this approach. Instead, the temperature and humidity profiles of the atmosphere are first retrieved, and then such data are used to calculate the various indices. This would ensure consistency among the various indices. Moreover, though there are various scanning methods of the radiometer, only the near-zenith mode data of the radiometer (elevantion angle of 79.8 degrees from the horizon) are considered here.

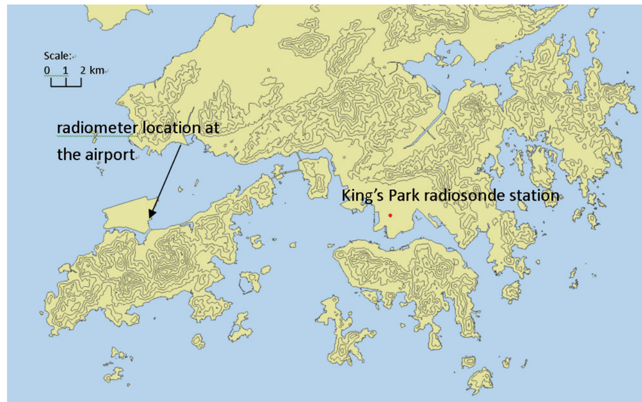

Figure 1: Locations of the weather stations as mentioned in the present study. Height contours of the terrain are in 100 m.

The temperature and the humidity data from the radiometer are available at specific heights above ground level, namely, 0 m, 10 m, 30 m, 50 m, 75 m, 100 m, 125 m, 150 m, 200 m, 250 m, 325 m, 400 m, 475 m, 550 m, 625 m, 700 m, 800 m, 900 m, 1000 m, 1150 m, 1300 m, 1450 m, 1600 m, 1800 m, 2000 m, 2200 m, 2500 m, 2800 m, 3100 m, 3500 m, 3900 m, 4400 m, 5000 m, 5600 m, 6200 m, 7000 m, 8000 m, 9000 m, and 10000 m. The pressures are determined from the surface pressure as well as the heights and temperatures at the various levels using hydrostatic approximation.

3 Comparison with radiosonde data

First of all, the quality of the radiometer-derived indices is studied by comparing with those derived from the nearly simultaneous measurements from the radiosonde, namely, the time (within 10 minutes) of the radiometer closest to the actual radiosonde observation at the relevant height is considered. The radiometer is located at the Hong Kong International Airport (HKIA) in the present study, which is about 25 km to the west of the radiosonde station at King's Park in Hong Kong (Fig. 1). The upper-air ascent measurements are only made available twice a day, namely, 00 and 12 UTC. The study period covers one year, namely, June 2008 to May 2009.

The comparison results are given in Fig. 2. In general, the radiometer-based and the radiosonde-based indices are well correlated. The correlation is the highest for HI (R^2 of about 0.70) and the worst for TT (R^2 of about 0.44). The standard errors are –0.83 and –5.02 respectively. The correlation coefficient squared at the various scatter plots are generally less than that reported for KI in CHAN (2009). This may be due to the relatively large separation between the two instruments in the present study. In CHAN (2009), the radiometer was

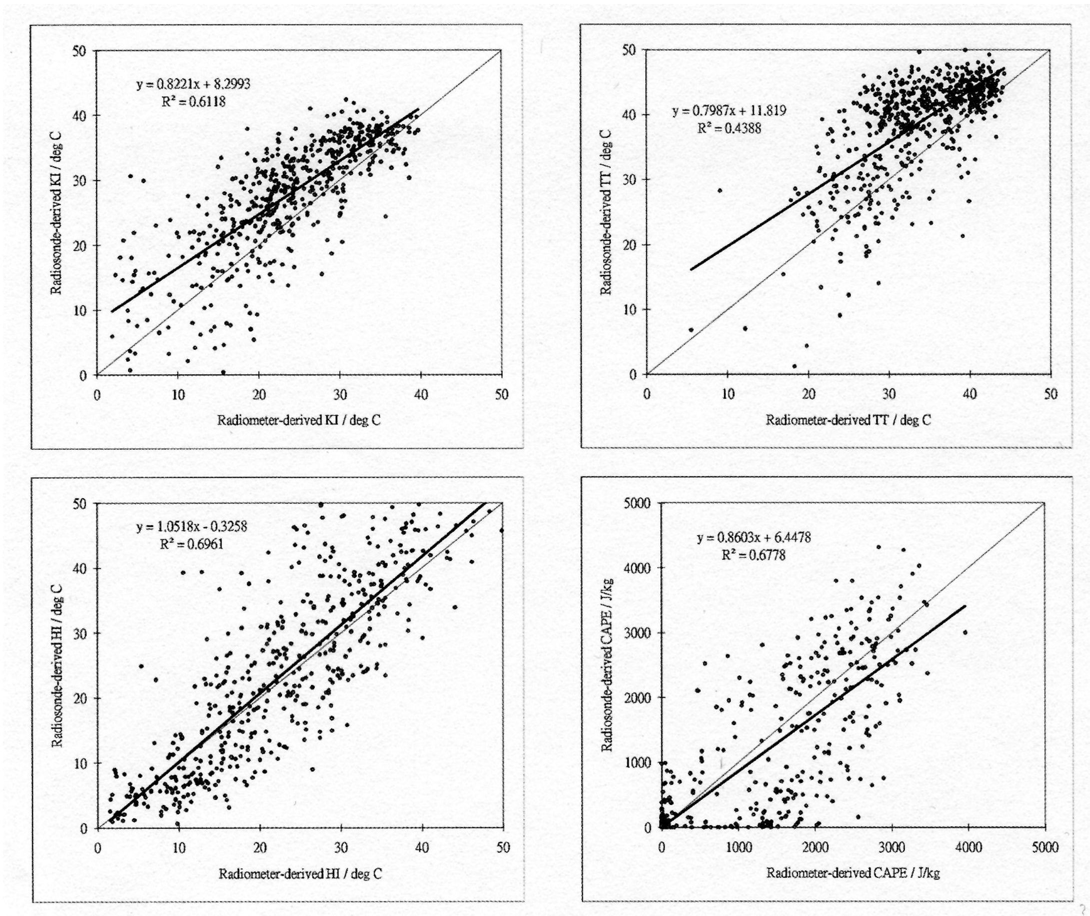

Figure 2: Comparison of the instability indices derived from the radiometer and radiosonde: K index, TT, HI and CAPE.

located at about 1 km south from the radiosonde station. In that study, the period under consideration was just the summer of one year only, and the correlation coefficient squared (R^2) was 0.733 for KI.

4 Frequency distributions of the stability indices in capturing lightning strokes

The performance of the various indices in capturing lightning strokes is established by examining the frequency distributions of the indices in "clear periods" and "lightning periods". The radiometer data updated every 10 minutes are studied here. The 10-minute intervals centred at the radiometer observation times are considered. This 10-minute interval is defined as a "period". As an indication of the convective instability, the cloud-to-ground lightning strokes from the lightning location information system (LLIS) over southern China are considered. According to the manufacturer, the LLIS has a position accuracy of less than 1 km and the detection efficiency is about 90 % inside and around Hong Kong. As a start, a distance of 50 km from the radiometer is adopted. If there is at least one lightning stroke within this 50-km radius of the radiometer in the 10-minute interval, it is regarded as a "lightning period". Otherwise, it is defined as a "clear period". Apart from the 50-km range, the radii of 30 and 90 km centred at the radiometer have also been considered and the frequency distributions look generally similar (not shown).

To study the seasonal behaviour of the frequency distributions, two study periods have been considered in this paper, namely, (a) June 2008 to August 2008 and May 2009, which is taken to be summer time, and (b) September 2008 to April 2009, which is taken to be non-summer time.

The frequency distributions in the summer time are shown in Fig. 3. The results for KI, TT and HI give slightly different thresholds of convective instability as adopted in literature, namely, KI value of 30 (vs. 20), TT value of 40 (vs. 30) and HI value of 10 (vs. 30) may be used as thresholds. (It is, however, noted that the threshold values for KI and HI are quite similar to those reported in WALKER et al. (2008).) The frequency distributions of "clear periods" and "lightning periods" show some degree of over-lapping. In general, the "clear periods" have wider distributions of index values, whereas the index distributions of "lightning periods" are narrower. The distinction of the two kinds of weather is par-

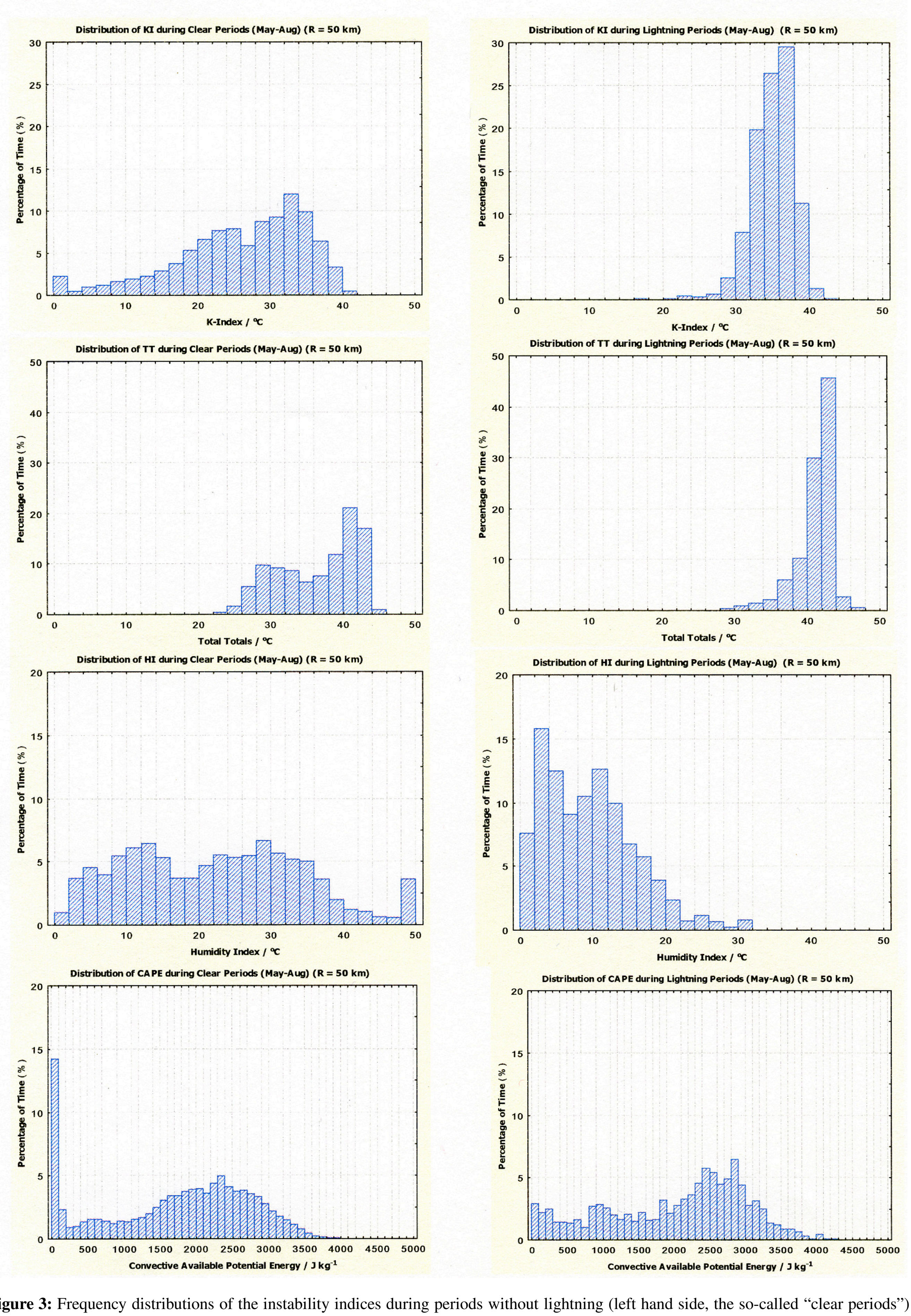

Figure 3: Frequency distributions of the instability indices during periods without lightning (left hand side, the so-called "clear periods") and with lightning (right hand side, the so-called "lightning periods"). From top to bottom: K index, TT, HI and CAPE.

ticularly poor for HI. On the other hand, for CAPE and SF (not shown), the distinction between the frequency distributions of "clear periods" and "lightning periods" is not so trivial. For each index, the distributions in these two kinds of periods look similar in term of the range of index values and the frequency values themselves. Based on these results, it appears that those instability indices calculated from the specific heights of the temperature/dew point profiles are more skillful in distinguishing between lightning and non-lightning situations, at least for the climatological conditions in Hong Kong.

5 Thresholds for lightning stroke occurrence based on relative operating characteristic (ROC) diagrams

The performance of radiometer-based indices in the indication of tropospheric instability could also be studied using ROC diagrams. For each particular index, the threshold for indicating convectively unstable atmosphere is varied. For a specific threshold value of the index, if the index meets the criteria and a lightning stroke occurs within 30 km from the radiometer in the 10 minute interval centred at the radiometer observation time, this event is taken to be a hit. Otherwise, if the index meets the criteria but there is no lightning stroke within 30 km, the event is taken to be a false alarm. The data of summer time and non-summer time are considered in calculating the probability of detection (POD) and probability of false detection (POFD) of the various index thresholds.

The resulting ROC curves are shown in Figs 4(a) to (e). There are a number of observations:

(a) The indices based on temperature/dew point values at specific heights are more skillful than CAPE and SF. This could be seen more clearly in the area under the ROC curves as shown in Fig. 4(f).

(b) In general, the indices are more skillful in the non-summer time than the summer-time, i.e. where the ROC curves get closer to the "ideal situation" at the upper left corner of the plot. This is also shown in the area under the ROC curves in Fig. 4(f). It appears that, in the summer time, the atmosphere may remain convectively unstable for extended periods of time, but there may be lightning or no lightning within each period, making the indices less skillful in correlating with the occurrence of lightning.

(c) For non-summer time, in order to achieve optimum performance (i.e. the intersection between the ROC curve and the "optimal performance" straight line from the upper-left corner to the lower-right corner of the plot), a higher threshold may be adopted for KI (29 vs. common value of 20) and TT (38 vs. common value of 30), and a lower threshold may be adopted for HI (17 vs. common value of 30). Similarly, in the summer time, a higher threshold may be adopted for KI (34) and TT (41), and a lower value for HI (13).

(d) The probability of detection of the various indices for summer/non-summer seasons are: 88 %/77 % for KI, 82 %/68 % for TT, 81 %/72 % for HI, 59 %/42 % for SF and 65 %/55 % for CAPE.

As shown in the above, the radiometer provides useful data in establishing the use of instability indices in the nowcasting of the occurrence of lightning strokes within a certain distance from the radiometer. The performance of the various instability indices is established with ROC curves, which may not be possible based on radiosonde data because of the much lower frequency of the availability of radiosonde data on a day and the rapid variation of the thermodynamic state of the troposphere. Based on the results of the present study, it appears that the instability indices as derived from temperature and humidity values at specific heights could be the most useful in indicating the occurrence of lightning strokes, at least for the climatological condition in Hong Kong.

6 Correlation between number of lightning strokes and instability index value

The correlation between the radiometer-derived instability index and the occurrence of lightning stroke is studied in the present section. In this section, we try to study the correlation of the indices with the number of lightning strokes occurring within a certain distance from the radiometer. This kind of study has been conducted before in CHAN (2009), based on one index only (namely, KI) and data of a limited period (early summer of one year). A similar study is repeated here, with more indices considered, data covering a much longer period (one whole year), and using a more objective way to establish a lightning episode.

In this paper, a lightning episode is defined as a period of 10 minutes or longer (multiples of 10 minutes) in which the total number of lighting strokes within a certain distance from the radiometer in each 10-minute interval of this period is at least 20. An example of a lightning episode, together with the time series of the various radiometer-based instability indices, is shown in Fig. 5. As a preliminary study, we choose the number of lightning strokes to be 20 in order to collect sufficient data sample (c.f. the situation of considering the number of lightning strokes in the order of a hundred, in which the number of cases considered would be rather small) and to remove those cases with isolated lightning strokes only (c.f. the situation of considering a few lightning strokes only [say, less than 10], in which the thunderstorm could be quite far away [e.g. more than 10–20 km away] in producing those few lightning strokes in the region under consideration). The number of lightning strokes could be varied in a future study to find out the sensitivity of the results as presented in this section.

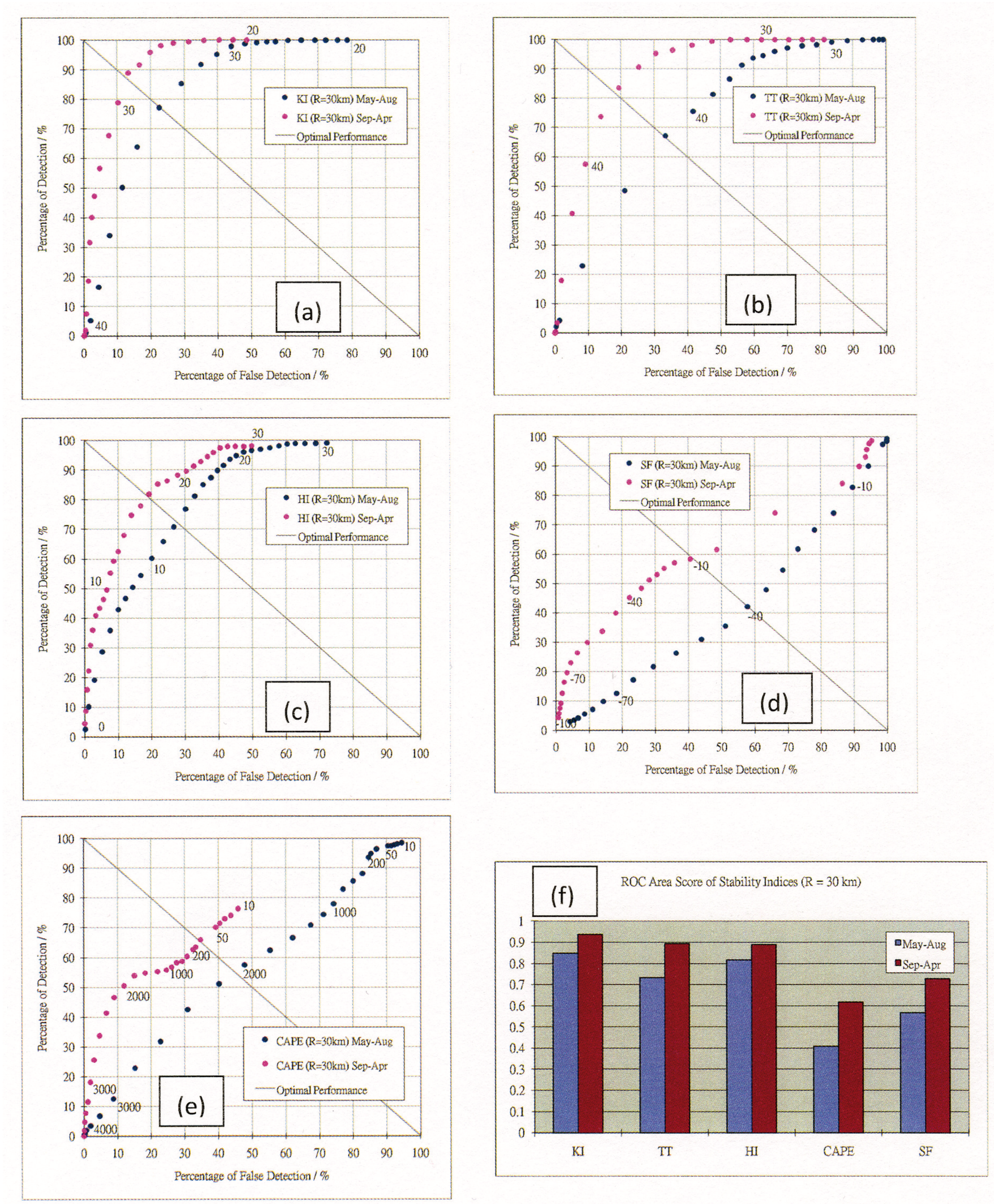

Figure 4: (a) to (e) are the ROC curves for various radiometer-based instability indices for summer (May to August) and non-summer (September to April) periods, including K index, TT, HI, SF and CAPE. (f) gives the areas under the ROC curves.

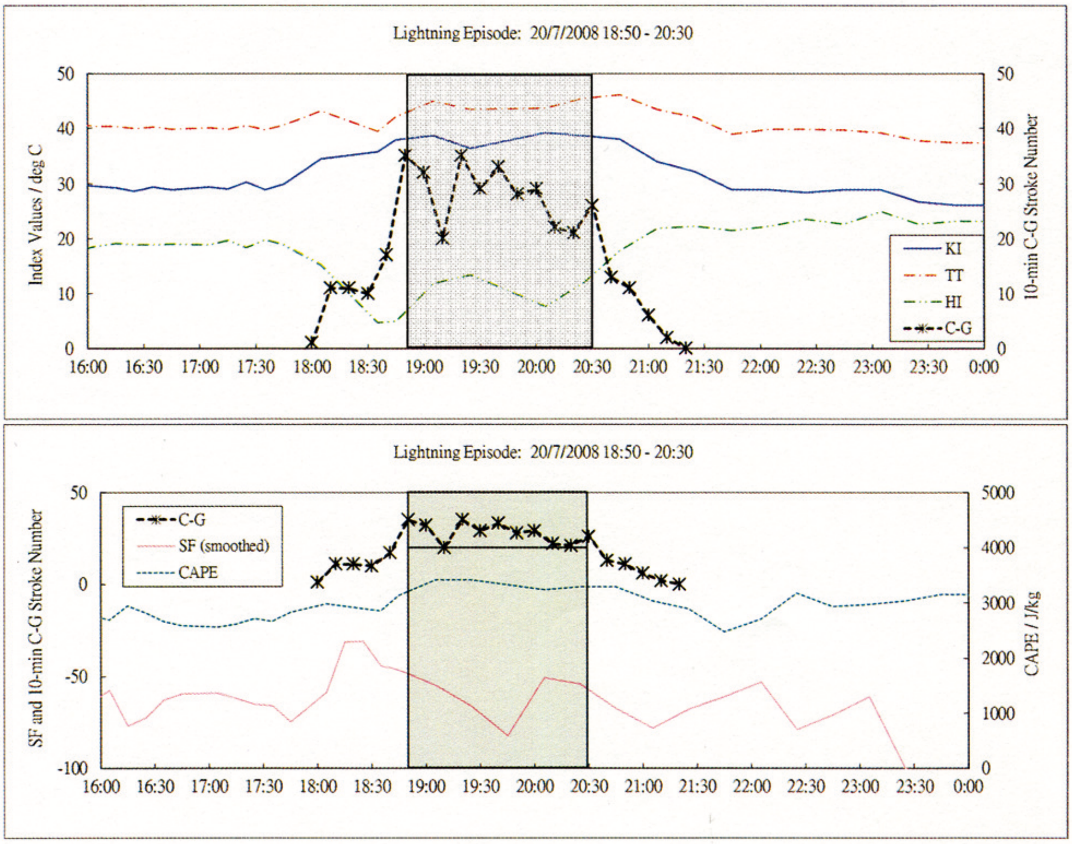

Figure 5: Time series of the number of cloud-to-ground lightning strokes and the values of the various instability indices for the sample lightning case of 20 July 2008. Upper panel: KI, TT and HI; lower panel: SF and CAPE. The "lightning episode" is highlighted in grey.

After considering all the indices, it turns out HI has the best correlation with the total number of lightning strokes. Fig. 6 shows that scatter plot between the minimum HI within the lightning episode and the logarithm of the total number of lightning strokes within a distance of 30 km from the radiometer. The same radius of 30 km as considered in Section 5 is adopted here. As could be expected from the definition of HI, as the minimum value of HI decreases, the atmosphere is more humid and thus the total number of lightning strokes increases. The correlation coefficient squared is less than that in a similar study before (CHAN, 2009), probably because more cases (data over a year) are considered in the present paper.

The above correlation for minimum value of HI is studied by considering lightning strokes within different distances away from the radiometer, viz. from 10 km to 90 km. The variation of the correlation coefficient of the resulting scatter plot with the distance from the radiometer is shown in Fig. 7. It turns out that the correlation coefficient is the highest at about 30 km. This is in generally the same order of magnitude for the distance considered in the study of frequency distributions and ROC curves of the instability indices above. The present study result is also consistent with that reported

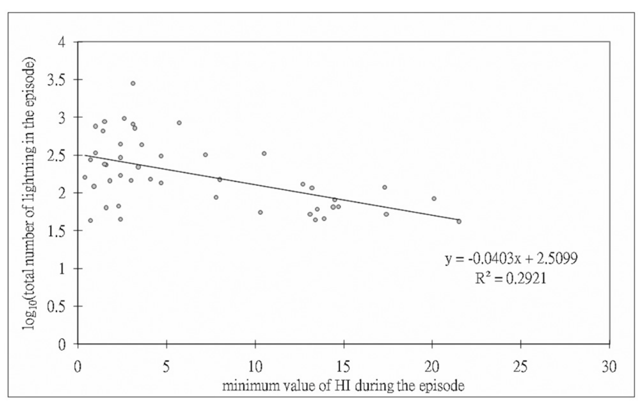

Figure 6: The scatter plot of logarithm of the total number of lightning strokes in the episode against the minimum value of HI during the episode with the distance of 30 km from the radiometer.

in CHAN (2009), namely, in terms of the correlation with the number of lightning strokes (as a proxy of the tropospheric instability), the ground-based microwave radiometer may be considered to be making measurements representative over a distance of about 30 km away.

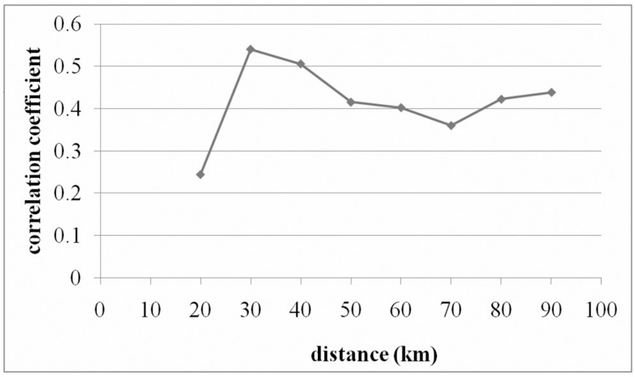

Figure 7: The variation of the correlation coefficients for the scatter plots similar to Figure 6 with the distances over which lightning strokes are counted. Here correlation coefficient (R) is considered instead of correlation coefficient squared (R^2).

7 Conclusions

The performance and application of radiometer-derived instability indices are studied in the present paper. First of all, the radiometer-derived indices are compared with those obtained from the radiosonde data. They are found to have high degree of correlation with each other. This establishes the quality of the radiometer-derived indices. The correlation is the highest for HI, with the correlation coefficient squared of about 0.70. This is considered good in view of the separation of the measurement locations (about 25 km) and the different principles of measurements (volume integral above a fixed location on the ground for radiometer vs. point measurement of a drifting balloon for radiosonde).

The study then continues with the correlation between the instability indices and the occurrence of lightning strokes within a certain distance from the radiometer (for lightning period, a threshold of 1 discharge is used). It turns out that, in the frequency distribution of the instability indices, there are some degrees of overlapping between the "clear period" and the "lightning period". Based on the frequency distributions, it is possible to derive a threshold for distinguishing between "clear period" and "lightning period" for each instability index. The thresholds so determined are comparable but not the same as the values as adopted in the literature. Such thresholds could also be established using ROC curves. It turns out that the instability indices are in general more skilful in winter months than in summer months. Moreover, the indices based on temperature and humidity at specific levels are more skilful in capturing the occurrence of lightning stroke than other indices like CAPE and SF. KI shows the best performance with probability of detection of 88 % and 77 % for non-summer and summer seasons respectively.

The next step is to establish any correlation between the instability index and the amount of lightning strokes (within a certain distance from the radiometer). For this purpose, a lightning episode is defined using a threshold of 20 discharges. It turns out that the correlation is the best using the minimum value of humidity index, with correlation coefficient of 0.55. The distance from the radiometer considered is about 30 km (having the best correlation between the number of lightning discharges and the instability index), which may be taken as the area over which the radiometer's measurement is considered to be representative of the atmospheric conditions.

It has been pointed out that one major limitation of the results presented in the paper is the bias and considerable spread in the instability indices derived from the radiometer and those from the radiosonde in the scatter plots in Fig. 2. First of all, the radiometer and the radiosonde are not co-located in the present study, namely, the radiosonde site is about 25 km to the east of the radiometer at the airport. The temperature and the humidity profiles from the two locations could be very much different from each other. Secondly, the measurement principles of the two instruments are different, namely, volume measurement of radiometer vs. point measurement of radiosonde. Though there are biases and spreads of the data points, the two datasets are found to have good correlation with each other. In other words, the radiometer-based instability index and the radiosonde-based instability index show similar trends with the evolution of the weather. As long as the radiometer is giving temperature and humidity profiles following the trend of the evolution of the atmospheric condition, the radiometer data at least have the potential for monitoring the stability of the troposphere and thus the chance of occurrence of intense convective weather. This point may be justified by the rather large areas under the ROC curves in Fig. 4(f), reaching above 0.8 for the radiometer-based indices like KI.

The thresholds developed for the radiometer-based instability indices in the present study may be specific to the microwave radiometer used. They may not be applicable to the radiosonde-based instability indices, in view of the biases and spreads of the data points in the scatter plots in Fig. 2. Nonetheless, these specifically determined thresholds, though may not be universally applicable to other radiometers with different hardware and retrieval algorithms and to other climatological conditions, could be applied to the continuously available instability indices available from the microwave radiometer in use and for the weather situations in Hong Kong for the purpose of monitoring the occurrence of intense convective weather. This paper is not meant to establish universal thresholds of instability indices for nowcasting of convective weather, but to demonstrate the methodology of establishing such thresholds for the application of microwave radiometer. This method could be applied to other radiometers and other climatological conditions.

The results in the present paper are preliminary. There are a number of research directions that could be pursued in future studies:

(a) Using a much larger dataset, especially multi-year dataset, and see if there is year-to-year variability of the results presented in this paper;

(b) Considering other instability indices commonly adopted for nowcasting of severe weather, such as lifted index;

(c) Better establishing the quality of the radiometer-based instability index using radiosonde data with the two kinds of instrument being closer together; this point is to improve on the present limitations in the comparison between the radiometer-based instability indices and the radiosonde-based instability indices, which have considerable spreads and biases in the scatter plots in Fig. 2;

(d) Studying the sensitivity of the correlation results in Sections 4 and 5 to the number of lightning strokes as defined in the "lightning period", for instance, at least 10 lightning strokes (more frequent/less frequent lightning stroke events) are considered instead of just 1 stroke (yes/no events);

(e) Studying the sensitivity of the correlation results in Section 6 above to the number of lightning strokes considered in the lightning episode.

References

CHAN, P.W., 2009: Performance and application of a multi-wavelength, ground-based microwave radiometer in intense convective weather. – Meteorol. Z. **18**, 253–265.

MANZATO, A., 2003: A climatology of instability indices derived from Friuli Venezia Giulia soundings, using three different methods. – Atmos. Res. **67–68**, 417–454.

MARINAKI, A., M. SPILIOTOPOULOS, H. MICHALOPOULOU, 2006: Evaluation of atmospheric instability indices in Greece. – Advan. Geosci. **7**, 131–135.

MICHALOPOULOU, H., C. JACOVIDES, 1987: Instability indices for the Cyprus Area. – Meteor. Atmos. Phys. **37**, 153–158.

TUDURÍ, E., C. RAMIS, 1997: The environments of significant convective events in the western Mediterranean. – Wea. Forecast. **12**, 294–306.

WALKER, I., V. CHAKRAPANI, W. ELMAHBOUB, 2008: The development of a shape factor instability index to guide severe weather forecasts for aviation safety. – Meteor. Appl. **15**, 465–473.